

# Ion-cyclotron waves in Solar Coronal Hole

S. Doğan<sup>a,b,\*</sup>, E. R. Pekünlü<sup>a</sup>

<sup>a</sup>University of Ege, Faculty of Science, Department of Astronomy and Space Sciences, Bornova, 35100, İzmir, Turkey

<sup>b</sup>Theoretical Astrophysics Group, University of Leicester, Leicester, LE1 7RH, UK

---

## Abstract

We investigate the effect of the Plume/Interplume Lane (PIPL) structure of the solar Polar Coronal Hole (PCH) on the propagation characteristics of ion-cyclotron waves (ICW). The gradients of physical parameters determined by SOHO and TRACE satellites both parallel and perpendicular to the magnetic field are considered with the aim of determining how the efficiency of the ICR process varies along the PIPL structure of PCH. We construct a model based on the kinetic theory by using quasi-linear approximation. We solve the Vlasov equation for O VI ions and obtain the dispersion relation of ICW. The resonance process in the interplume lanes is much more effective than in the plumes, agreeing with the observations which show the source of fast solar wind is interplume lanes. The solution of the Vlasov equation in PIPL structure of PCH, the physical parameters of which display gradients along and perpendicular direction to the external magnetic field, is thus obtained in a more general form than the previous investigations.

*Keywords:* Sun: corona - solar wind - plasmas - waves - acceleration of particles

---

## 1. Introduction

The motivation for the present investigation is given by UVCS/SOHO measurements which showed the collisionless nature of the solar North Polar Coronal Hole (NPCH) (e.g. Cranmer et al. 1999; Kohl et al. 1999). What was seen in the Mg X and O VI line measurements was that the plasma in NPCH was collisionless beyond the 1.75 - 2.1  $R_{\odot}$  (Doyle et al. 1999). Kumar et al. (2006) took the dissipative terms like resistivity and viscosity into account and considered the parallel (to the magnetic field) heat conduction due to Coulomb collisions in order to investigate the coronal heating by MHD waves. All the efforts have been spent to account for the heating of the different parts of corona by wave-particle interactions.

Tu and Marsch (1997) developed a two-fluid MHD model of the solar corona and wind. In their model they investigated the effects of Alfvén waves, within the 1 Hz-1 kHz frequency range, on the heating and acceleration. They showed that their model can fit the observed density profiles of polar coronal hole and polar plume at 2.4  $R_{\odot}$  and 3.2  $R_{\odot}$ , respectively. They also obtained the solar wind speeds at 63  $R_{\odot}$ .

---

\*Corresponding author

Email address: [suzan.dogan@mail.ege.edu.tr](mailto:suzan.dogan@mail.ege.edu.tr) (S. Doğan)

Marsch and Tu (1997) investigated the heating and acceleration of the solar corona and the solar wind by considering Alfvén waves that are assumed to be produced by small scale reconnections in the chromospheric network. Their two-fluid model predicted that the Alfvén waves within the 200 Hz - 790 Hz frequency range damp inside  $1.5 R_{\odot}$  and thus heat the corona and accelerate the solar wind near the Sun.

Besides, NPCH is also structured in radial direction by so-called plume and interplume lanes (PIPL) (see, Figure 1 in Wilhelm et al. 1998). PIPL structure is taken into account by several authors in their investigation (e.g., Ofman et al. 2000). Upper chromosphere and the corona show anisotropic viscosity, resistivity and thermal conductivity. Ruderman et al. (2000) considered the damping of the slow surface waves propagating along the magnetic field in such a medium.

Lie-Svendsen et al. (2002) studied the solar wind in expanding coronal holes wherein the heat flux densities are along the magnetic field. By the accumulation of data on NPCH, it has been clear that the coronal hole heating by MHD waves should be considered in the *nonclassical* context, i.e., Coulomb collisions and Maxwell distribution of plasma species cannot and should not be assumed (Williams 1997).

It is a well-known fact that in such a medium like NPCH where the particle number density as well as the effective temperature of the plasma species have gradients both in the radial and the perpendicular direction to the line of sight (*los*) and the magnetic field has a gradient in radial direction, the wave propagation characteristics display novelties (e.g., Joarder et al. 1997). If the typical length scale of the wave is comparable to the length scales of the physical parameters of the medium MHD waves tend to refract towards resonance and go through collisionless damping (Melrose & McPhedron 1991).

Nakariakov et al. (1998), in dealing with the coronal heating processes of Sun and late type stars, considered nonlinear wave coupling in a MHD context. They retained the nonlinear terms in the x and z-components of the linearized momentum equation. They claimed that the nonlinear terms in their equations are to be held responsible for the generation of fast modes. They also cite their previous studies wherein they showed that the cause of the nonlinear generation of these fast waves are the longitudinal and transversal gradients in the magnetic pressure. Nakariakov (2006) considered the effects of transverse structuring in plumes and drew attention to the effect of different spatial scales of transverse and longitudinal inhomogeneities on the wave dynamics. We are agreed with Nakariakov and propose to take into account the gradients of physical parameters both in plume and interplume lanes.

Vocks & Marsch (2001) treated the wave-particle interaction within the framework of quasi-linear theory by solving the Vlasov equation numerically. They considered the heating process by a wave-particle interaction in a coronal funnel and in the lower corona up to a height of  $0.57R_{\odot}$ . Their Figure 1 shows that  $T_{\perp}$  for  $O^{5+}$  reaches about  $3 \times 10^7$  K at the upper part of the computational domain. They assumed dispersionless waves and put off the consideration of dispersive effects for a future investigation.

In the present investigation, we also solve the Vlasov equation in 2D one of which covers the distance range of  $1.5R - 3.5R$ , where  $R$  is the dimensionless radial distance, i.e.,  $R = r/R_{\odot}$  and the other is the x-direction perpendicular both to the radial direction and the *los* and the details of x is given in Subsection 2.1. Wave propagation characteristics in NPCH was investigated by Pekünlü et al. (2004). They did not take the PIPL structure of the medium into account. To the best knowledge of the authors of the present investigation the effect of PIPL structure of NPCH on the wave propagation characteristics has not been taken into account hitherto. This is our aim in this study. We should mention in passing that in our investigation, we take the observational parameters of NPCH into consideration. Nevertheless, the same conclusions we draw apply also

all the coronal holes be it as it may appear in the north or south. Since our model should be valid for polar coronal hole (PCH) in general, we will use the term PCH for our investigation.

Cranmer et al. (2008) list the three primary observables as the absolute intensity of the O VI  $\lambda 1032$  line, the line width  $v_{1/2}$  and the intensity ratio R of the  $\lambda 1032$  to the  $\lambda 1037$ , which depend on the four or “unknown” quantities along the *los* distribution, i.e., ion fraction  $n_{\text{OVI}}/n_e$ , the O VI bulk outflow speed along the magnetic field, and the parallel and perpendicular O<sup>5+</sup> kinetic temperatures. They refrain from making a definitive separation between  $T_i$  the ionization temperature and the nonthermal part of the effective temperature (see Eq. 1). They also draw attention to the necessity for new observations in order to make further progress and not to make arbitrary assumptions about, e.g., the ion outflow speed or the ion temperature. Kohl et al. (2006) showed that the plasma properties in NPCH remain reasonably constant about a year or two around solar minimum (1996-1997). This constancy of plasma parameters enables us to express them as a function of R and  $x$ .

Isenberg & Vosquez (2009) considered the cyclotron-resonant Fermi heating mechanism by taking into account the effects of gravity, charge-separation electric field, and mirror force in a radially expanding flux tube. They found that a small fraction of nonlinearly generated resonant wave power can provide the observed energization for O VI ions.

Devlen & Pekünlü (2010) investigated the effects of the O VI temperature and number density gradients in the parallel and perpendicular direction to the magnetic field in the MHD context. Their results show that the perpendicular (to the external magnetic field) heat conduction introduces novelty to the wave propagation characteristics.

The plan of the paper is as follows: In Section 2 we review the plasma properties of the NPCH revealed by SOHO and TRACE satellites. In Section 3, we assume that the coronal hole plasma is electrically *quasineutral*, that is,  $N_e \approx N_p \approx N$  where subscripts stand for electron and proton, respectively (Marsch 1999; Endeve & Leer 2001; Voitenko & Goossens 2002). Then, bearing in mind another observational fact that O VI ions are preferentially heated, we’ll obtain the dispersion relation of the ion cyclotron waves (ICW) in PIPL structure of the PCH by solving the Vlasov equation and present the summary and conclusion in Section 4. We use CGS units in this study.

## 2. NPCH Plasma Properties

### 2.1. O VI Ion Temperatures

Since the NPCH is collisionless and a typical low -  $\beta$  plasma, we expect that it shows temperature anisotropy. Indeed, O VI 1032 Å line intensities vary in the radial direction as well as in the direction both perpendicular to the radial and the *los* ones (Kohl et al., 1997a). Their Figure 16 shows that O VI line widths obtained from the darker interplume lanes are wider than the ones coming from the brighter plumes. SUMER observations also revealed that the line widths from interplume lanes are wider than those of plumes (Wilhelm et al. 2000; Banerjee et al. 2000, Banerjee et al. 2009a). The effective temperature of the O VI ions at 3.0 R is given as  $T_{\perp\text{eff}} \sim 10^8\text{K}$  (Cranmer et al. 1999). Antonucci et al. (2000) give the effective temperature profile of O VI ions in the 1.5 - 3.0 R. The relation between the ion temperature and the effective temperature is,

$$T_{\text{eff}} = (m_i/2k_B)v_{1/e}^2 = T_i + (m_i/2k_B)\xi^2 \quad (1)$$

where  $T_i$  is the ion temperature;  $m_i$  is the ion mass;  $k_B$  is the Boltzmann constant;  $v_{1/e}$  is the *los* speed;  $\xi$  is the most probable speed of an isotropic, Gaussian-distributed, turbulent velocity field

(Wilhelm et al. 1998). The relation between  $\xi$  and the wave amplitude is  $\xi^2 = (1/2)\langle\delta v^2\rangle$  (Esser et al. 1999). Doyle et al. (1999) report that for Alfvén-like waves “factor 2 accounts for the polarization and direction of propagation of a wave relative to the *los*”.

We follow the coup and do not make any assumptions about the ion temperature and the nonthermal part of the effective temperature but only stick to the observational fact that there is no temporal variation of the effective temperature within several time scales of ICW’s propagation in NPCH.

Banerjee et al. (2000) used the comprehensive and self-consistent empirical model of Cranmer et al. (1999) and derived a best-fit function for the O VI line width valid in 1.5-3.5 R (see their Eq. 3). We converted their Eq. 3 into the effective temperature as below,

$$T_{\text{eff}}(R) = 4.02 \times 10^7 R^2 + 1.25 \times 10^7 R - 9.76 \times 10^7 \text{ K.} \quad (2)$$

Since there is no data about the effective temperature of NPCH plasma and/or O VI ions along the *los* we assumed that *los* temperature of O VI ions is constant. Esser et al. (1999) showed that Mg X and O VI ion temperatures ( $T_i$ ) are much greater than the proton temperature. They also compared the ion temperatures of Mg X and O VI ions on various distances from the solar surface. For instance, they found that at 1.6 and 1.75  $R_\odot$ , O VI temperature is in the same range as  $T_{\text{MgX}}$ . But at 1.9 and 2  $R_\odot$   $T_{\text{OVI}}$  was found to be much higher than  $T_{\text{MgX}}$ . Ion temperatures ratio of these two minor ions displayed a minimum value of 1.6 at 1.9  $R_\odot$  and 1.32 at 2  $R_\odot$  and the maximum value of 13 at 1.9  $R_\odot$  and 6.6 at 2  $R_\odot$ . We used Fig. 2a in Esser et al. (1999) in order to find polynomial form for the radial profile  $\delta v_{\text{MgX}}$ . We tried hard to find a similar radial profile for O VI in the literature, but in vain. Therefore we adopt  $\delta v_{\text{MgX}}$  as if it is  $\delta v_{\text{OVI}}$  and derived the polynomial form of the nonthermal part of  $T_{\text{eff}}$  of O VI ions and designate it as  $T_{\text{eff}}^\xi$ :

$$T_{\text{eff}}^\xi = -2.48 \times 10^6 R^2 + 2.07 \times 10^7 R - 1.78 \times 10^7 \text{ K.} \quad (3)$$

Using  $\delta v_{\text{MgX}}$  profile to represent  $\delta v_{\text{OVI}}$  in our calculations surely introduces some imprecision to our results but it is less than, at most, and order of magnitude, so we did not refrain from adopting  $\delta v_{\text{MgX}}$  for  $\delta v_{\text{OVI}}$ . In Table 1 we present the variations of  $T_{\text{eff}}$ ,  $T_i$ ,  $T_{\text{eff}}^\xi$  and  $T_{\text{eff}}^\xi/T_i$  with the radial distance.  $T_{\text{eff}}$  is derived from the O VI line width (Banerjee et al. 2000; Cranmer et al. 1999);  $T_{\text{eff}}^\xi$  is from Esser et al. (1999). By using these values in Eq. (4) we obtained  $T_i$ .

Devlen & Pekünlü (2010) modeled the non-thermal part of the effective temperature of O VI ions in two dimension in NPCH (see Fig. 1). Wilhelm et al. (1998) report that the effective temperature of O VI ions in the interplume lanes are about 30% higher than that of the plumes. We derived the length scale of the effective temperature gradient perpendicular to both the radial direction and the *los* by referring to the Figure 1 of Wilhelm et al. (1998). They give the width of the PIPL structure of the NPCH at 1.03 R as 380”. At Sun, 1”  $\approx$  715 km. There appears four interplume lanes and four plumes in Figure 1 of Wilhelm et al. (1998). Although the widths of plumes and interplume lanes are unequal, we made a rough estimation and divided 380” by eight and assumed that they are equal in width. The average width of these plumes and interplume lanes turns out to be 33962.5 km. We take this value as the length scale ( $\Lambda_x^T$ ) of the perpendicular temperature gradient at 1.03 R. Between  $R = 1.034$  and  $R = 1.32$ , the widths of the plumes are reported to increase by a factor of 2 (Wilhelm et al. 1998). This observational fact enables Devlen & Pekünlü (2010) to formulate the temperature structure of NPCH in ( $R, x$ ) space as given by Eq. (4).

$$T_{\text{eff}}(R, x) = T_{\text{eff}}(R) + 0.3T_{\text{eff}}(R) \sin^2\left(\frac{2\pi}{\lambda}x\right) \quad (4)$$

Table 1: O VI Temperatures

| R<br>( $r/R_{\odot}$ ) | $T_{\text{eff}}$<br>(/ $10^7$ K) | $T_i$<br>(/ $10^7$ K) | $T_{\text{eff}}^{\xi}$<br>(/ $10^7$ K) | $T_{\text{eff}}^{\xi}/T_i$ |
|------------------------|----------------------------------|-----------------------|--|----------------------------|
| 1.5                    | 1.6                              | 0.80                  | 0.77                                   | 0.96                       |
| 1.6                    | 3.0                              | 2.1                   | 0.9                                    | 0.43                       |
| 1.7                    | 4.5                              | 3.5                   | 1.0                                    | 0.29                       |
| 1.8                    | 6.1                              | 5.0                   | 1.1                                    | 0.23                       |
| 1.9                    | 7.8                              | 6.5                   | 1.3                                    | 0.19                       |
| 2.0                    | 9.5                              | 8.2                   | 1.4                                    | 0.17                       |
| 2.1                    | 11.4                             | 9.9                   | 1.5                                    | 0.15                       |
| 2.2                    | 13.3                             | 11.7                  | 1.6                                    | 0.13                       |
| 2.3                    | 15.3                             | 13.7                  | 1.7                                    | 0.12                       |
| 2.4                    | 17.4                             | 15.7                  | 1.8                                    | 0.11                       |
| 2.5                    | 19.6                             | 17.8                  | 1.8                                    | 0.10                       |
| 2.6                    | 21.9                             | 20.0                  | 1.9                                    | 0.10                       |
| 2.7                    | 24.2                             | 22.2                  | 2.0                                    | 0.09                       |
| 2.8                    | 26.7                             | 24.6                  | 2.1                                    | 0.08                       |
| 2.9                    | 29.2                             | 27.0                  | 2.1                                    | 0.08                       |
| 3.0                    | 31.8                             | 29.6                  | 2.2                                    | 0.07                       |
| 3.1                    | 34.5                             | 32.2                  | 2.3                                    | 0.07                       |
| 3.2                    | 37.2                             | 34.9                  | 2.3                                    | 0.07                       |
| 3.3                    | 40.1                             | 37.8                  | 2.4                                    | 0.06                       |
| 3.4                    | 43.0                             | 40.7                  | 2.4                                    | 0.06                       |
| 3.5                    | 46.1                             | 43.6                  | 2.4                                    | 0.06                       |

Effective temperature ( $T_{\text{eff}}$ ), ion temperature ( $T_i$ ) and the non-thermal part of the effective temperature ( $T_{\text{eff}}^{\xi}$ ) of O VI ions are listed as a function of radial distance (R).

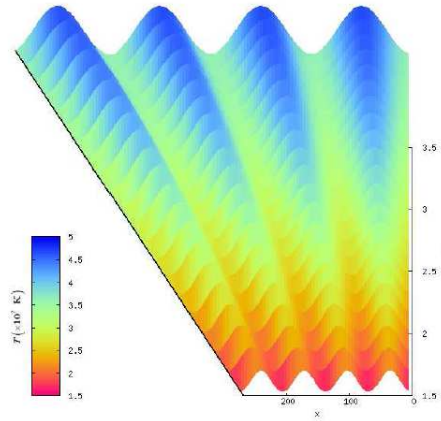


Figure 1: Non-thermal part of the effective temperature of O VI ions in NPCH as a function of R and x. The crests corresponds to the interplume lanes and the troughs to the plumes. The width of the PIPL varies with R. The abscissa x is in arcseconds as it is also in Wilhelm et al. (1998). From Devlen & Pektinli (2010).

where  $x$  is the direction perpendicular both to  $R$  and  $los$  and  $\lambda$  is the expansion rate of the widths of the PIPL in NPCH in arc seconds, i.e.,  $\lambda = 92''.16R$  (see Fig. 1).  $\lambda$  also represents the wavelengths of the  $\sin^2(2\pi x/\lambda)$  function which is a function of  $R$  and  $x$ . The factor 0.3 comes from the difference between the plume and interplume lane temperatures (30% max.). In that case, the effective temperature gradient of O VI ions in two dimensions can be expressed as below (Devlen & Pekünlü, 2010):

$$\nabla T_{\text{eff}}^{\xi}(R, x) = \frac{\partial T_{\text{eff}}^{\xi}}{\partial R} \widehat{\mathbf{R}} + \frac{\partial T_{\text{eff}}^{\xi}}{\partial x} \widehat{\mathbf{x}} \quad (5)$$

where  $\widehat{\mathbf{R}}$  and  $\widehat{\mathbf{x}}$  are the unit vectors of the above-defined  $R$  and  $x$  directions.

We should mention, in passing, that the temperature structure in  $x$ -direction could be modelled in various ways. We could choose the Heaviside step function, for example, instead of  $\sin^2(2\pi x/\lambda)$  but refrained from assuming a jumpy passage to a 30% higher temperature from plumes to interplume lanes and vice versa.

## 2.2. Number Densities in NPCH

Electron number density distributions in the north and south polar coronal holes are given by Fisher and Guhathakurta (1995). If the values they report are typical for the plumes then the analytical expression for electron number density distribution may be given as below (Esser et al. 1999):

$$N_e^{\text{PL}}(R) = 2.494 \times 10^6 R^{-3.76} + 1.034 \times 10^7 R^{-9.64} + 3.711 \times 10^8 R^{-16.86} \text{ cm}^{-3} \quad (6)$$

where the superscript PL stands for plume. Marsch (1999), Endeve & Leer (2001) and Voitenko & Goossens (2002) regard the coronal hole plasma as *quasineutral*, i.e.,  $N_e \approx N_p \approx N$ . Raymond et al. (1997) obtained the abundances of oxygen and other elements in coronal streamers. They found an oxygen number density  $N_{\text{OVI}} = 6.8 \times 10^{-5} N_p$  for the streamer center. Ciaravella et al. (1999) also observed a coronal streamer and obtained  $N_{\text{OVI}} = 5.9 \times 10^{-4} N_p$ . In the model for the kinetics of ions in the solar corona, Vocks (2002) chose the oxygen density as  $N_{\text{OVI}} = 10^{-3} N_p$ . Finally, in a recent study, Cranmer et al. (2008) give the upper and lower values of O VI number densities in polar coronal holes  $N_{\text{OVI}} = 2.4 \times 10^{-6} N_p$  and  $N_{\text{OVI}} = 8 \times 10^{-7} N_p$ , respectively. Taking a simple average they have a mean value of  $N_{\text{OVI}} = 1.52 \times 10^{-6} N_p$ . Since the observational uncertainty on the O VI abundances in NPCH still persists, we'll use the highest and the lowest values for O VI number density, i.e.,  $N_{\text{OVI}} = 10^{-3} N_p$  and  $N_{\text{OVI}} = 1.52 \times 10^{-6} N_p$  in our calculations in Section 3 to see how sensitive the wave propagation characteristics is to the O VI abundance. We should mention in passing that Cranmer (2000), Cranmer et al. (1999) and Tu & Marsch (1999) showed that minor ion species can dissipate the ICWs faster than the more abundant ones.

Cranmer et al. (1999) used the mean electron density in coronal holes, in other words, they derived the analytical form of the electron density by averaging over plumes and interplume lanes. However, number densities of electrons in plumes appear to be 10% higher than that of interplume lanes (see, e.g. Kohl et al. 1997a). Since we assume, in the light of observational data, that  $N_e \approx N_p$ , then the number density of protons in  $(R, x)$  plane becomes (Devlen & Pekünlü, 2010),

$$N_p(R, x) = N_p^{\text{PL}}(R)[1 - 0.1 \sin^2(2\pi x/\lambda)] \text{ cm}^{-3} \quad (7)$$

Here the factor 0.1 comes from the difference of the number densities between plumes and interplume lanes. If we should adopt the *quasineutral* assumption then the O VI number density may be expressed as below. Subscript  $i$  stands for O VI (Devlen & Pekünlü, 2010).

$$N_i(R, x) = fN_p^{\text{PL}}(R)[1 - 0.1 \sin^2(2\pi x/\lambda)] \text{ cm}^{-3} \quad (8)$$

where  $f$  will assume values  $1.52 \times 10^{-6}$  as given by Cranmer et al. (2008) or  $10^{-3}$  as adopted by Vocks (2002) in his model. For the purpose of detecting Alfvén waves in PCHs through EUV line width variations, Banerjee et al. (2009b) used EIS/Hinode spectrometer. The authors studied the electron number density variation with nonthermal velocity for PCH. An interested reader may refer to their Figure 5 in the above-cited article.

### 2.3. Magnetic Field in NPCH

To the best knowledge of the authors of the present investigation, there is no indication in the literature of this field, as to whether the magnetic field shows any spatial variation in  $x$  direction, therefore heliocentric distance dependence of NPCH magnetic field given by Hollweg (1999a) will be used in the next section:

$$B = 1.5(f_{\text{max}} - 1)R^{-3.5} + 1.5R^{-2} \text{ Gauss} \quad (9)$$

where  $f_{\text{max}} = 9$ . This model is valid in the range 1.0 - 10.0 R which covers the range we are interested in, i.e. 1.5 - 3.5 R. O VI cyclotron frequency's ( $\omega_c = q_i B/m_i c$ ) radial dependence will be calculated by using the Eq. (9).

### 2.4. Ion - Cyclotron Waves (ICW) in PCH

ICW may be generated by various mechanisms in various parts of the PCH. We do not touch upon the wave generation mechanisms, but simply take ICW for granted. Generation of resonant ICW may be possible by stochastic magnetic foot point motions, magnetic reconnections and MHD filamentation instabilities or from MHD turbulent cascade. This latter mechanism is supposed to be the dominant one producing ICW that heat the coronal hole plasma and accelerate the solar wind particles (Cranmer 2000). Axford et al. (1999) suggest that these waves may be generated by turbulent cascade from low to high frequencies or directly. Gupta et al. (2010), using EIS/Hinode and SUMER/SOHO data, detected propagating disturbances in coronal lines in plume and interplume lanes. They concluded that the waves are probably either Alfvénic or fast magnetoacoustic in the interplume regions and slow magnetoacoustic in plumes. Tomczyk et al. (2007) detected Alfvén waves by using Coronal Multi-Channel Polarimeter (CoMP) at the National Solar Observatory, New Mexico. Observations showed the existence of upward propagating waves with phase velocity  $1 - 4 \times 10^6$  m/s. They concluded that the waves are too weak to heat the solar corona and added that the unresolved Alfvén waves may carry enough energy to heat the corona. Doorselaere et al. (2007) appraised the observation of Alfvén waves by Tomczyk et al. (2007) as an important new progress in coronal physics. The important point in this context is as to whether the wave flux density of the ICW is high enough to replace the energy lost by thermal conduction to the transition region and the optically thin emission. A recent evaluation of the wave energy flux is given by McIntosh et al. (2011). By using the SDO/AIA image sequences and applying Monte Carlo simulations, the authors measured the amplitudes, periods and phase speeds of transverse waves. They concluded that the estimated energy flux in the quiet corona and coronal holes could supply the energy needed for fast solar wind in two stages: at the

first stage, injected plasma from lower part of the atmosphere heats the coronal base and at the second stage Alfvénic waves dissipate and accelerate the solar wind in PCH.

Energy flux density of the ICW is given as (e.g., Banerjee et al. 1998),

$$F_{\omega} = \sqrt{\rho/4\pi} \langle \delta v^2 \rangle B \text{ ergcm}^{-2}\text{s}^{-1} \quad (10)$$

The wave amplitude at heights 120'' off the solar limb is about,  $\langle \delta v^2 \rangle = 2 \times (43.9 \text{ kms}^{-1})^2$ . Adopting the values for  $B = 5 \text{ G}$  and  $N_e = 4.8 \times 10^{13} \text{ m}^{-3}$  at  $r = 1.25 \text{ R}$ , Banerjee et al. (1998) found the wave flux density as  $F_{\omega} = 4.9 \times 10^5 \text{ ergcm}^{-2}\text{s}^{-1}$  which is high enough for the ion-cyclotron resonance (ICR) process to be a good candidate for heating the coronal hole.

We may assume that the most favorable process for heating the NPCH is the ICR process. We may justify this assumption on the ground of two observational facts: a) Doppler dimming analysis (Kohl et al. 1997a) showed that the perpendicular (to the magnetic field) temperature of the O VI ions is about two order of magnitude higher than the parallel one, i.e.,  $T_{\perp} \sim 10^2 T_{\parallel}$  and b) outflow velocities in the solar wind of O VI ions in the interplume lanes are higher than that of the lanes. The seat of the fast solar wind was identified as the interplume lanes (Wilhelm et al. 1998; Hollweg 1999a, 1999b, 1999c). This shows that the ions having greater perpendicular velocities will experience a higher mirror force,  $F_{\text{mf}}(R) = -\mu \nabla B = -[(1/2)m_i v_{\perp}^2 / B(R)] \nabla B$ . These two effects could be brought about only by ICR process (Hollweg 1999a, 1999b, 1999c).

Therefore the ICR process is regarded as the most efficient heating mechanism for PCH. Observations also show that whatever the heating mechanism, O VI ions are preferentially selected (Kohl et al. 1997b). Alfvén waves undergoing the ICR process and dissipating their energies was examined by Cranmer (2000). One has to refer to this paper for earlier work in this field. In Section 3 we present our model based on the observational results presented in this section.

### 3. Solution of the Vlasov Equation in PIPL structure of PCH

We consider the wave equation derived for a cold plasma. In order to justify the *cold plasma* approximation, we should point out that two conditions are to be fulfilled in PCH: a) perpendicular wavelength should be greater than O VI ion Larmor radius ( $k_{\perp} v_{\perp} / \omega_c \ll 1$ ) and b) parallel phase velocity of ICW should be larger than the O VI ion thermal velocity ( $v_{\parallel} \ll \omega / k_{\parallel}$ ) (Schmidt, 1979). We assume a quasi-parallel propagation, in the sense that  $k_{\perp} / k_{\parallel} \ll 1$ , in PCH, therefore the former condition is readily fulfilled. The latter condition will be shown satisfied *a posteriori*. We assume that the perturbed quantities variation in space and time is like a plane wave, i.e.,  $\exp[i(\mathbf{k} \cdot \mathbf{r} - \omega t)]$ , where  $\mathbf{k}$  is the wave vector,  $\mathbf{r}$  is the distance from the source,  $\omega$  is the wave frequency and  $t$  is the time. In our investigation, we'll not take the  $\cos \theta$  factor in  $\mathbf{k} \cdot \mathbf{r} = |\mathbf{k}| |\mathbf{r}| \cos \theta$ , where  $\theta$  is the angle between the wave vector and the magnetic field. It is implicit in the above given condition, i.e.,  $k_{\perp} / k_{\parallel} \ll 1$ , that we may assume a quasi - longitudinal propagation but not forgetting the fact that we need  $k_{\perp}$  so that the refraction of the waves can cause communication between the adjacent flux tubes in plumes and interplume lanes. Murawski et al. (2001) also modeled the coronal hole as a cold plasma slab but with a uniform magnetic field. Written in terms of Fourier components, the wave equation is as below (e.g., Stix 1962, 1992),

$$\mathbf{k} \times (\mathbf{k} \times \mathbf{E}) + \frac{\omega^2}{c^2} \boldsymbol{\kappa} \cdot \mathbf{E} = 0 \quad (11)$$

where  $\boldsymbol{\kappa}$  is the dielectric tensor and will be derived from the Vlasov equation. O VI ions will be considered under the two forces, a) Lorentz force,  $q[\mathbf{E} + \frac{1}{c}(\mathbf{v} \times \mathbf{B}_0)]$  where  $\mathbf{E}$  is the electric field of



the ICW waves and  $\mathbf{B}_0$  is the external magnetic field of the PCH and b) pressure gradient force,  $-\nabla p$ .

Before proceeding with the linearization of the Vlasov equation we should discuss the justifiability of the pressure gradient term in the Vlasov equation.

The Vlasov equation usually does not contain the pressure gradient term. More recently, Tronci (2010) mentions so-called “hybrid kinetic-fluid models” and argues that, “These models are usually realized by following a hybrid philosophy that couples ordinary fluid models to appropriate kinetic equations governing the phase-space distribution of the energetic particle species”(see Eq. 70 in Tronci’s paper).

Cheng (1991) argues that plasmas in a large magnetic fusion devices as well as in space can be considered as having two components: the background one with a low energy which satisfies the fluid description (MHD) and the energetic one with a low density which should be treated by the kinetic approach. Cheng (1999) further proposed the extension of the kinetic-MHD model by properly including important kinetic effects of all the plasma species.

Another example reveals itself in the astrophysical literature dealing with the plasma instabilities in clusters of galaxies (Schekochihin et al., 2005). The authors of this study include the pressure gradient term in the Vlasov equation (see their Eq. 5) and cite Kulsrud (1983). This paper is different from Tronci’s (2010) one in the sense that there are no velocity moment equations (i.e., MHD equations) coupling to the Vlasov equation.

Cranmer (2002) identifies the thermal pressure gradient in the hot corona as the dominant outward force on particles in both fluid and kinetic models and notes that “*this force is a completely collisionless phenomenon*”. This unconventional description of pressure gradient force combined with the observational data clearly show that both the density and the temperature of O VI ions are the functions of radial distance from the Sun and along the x - direction. Thermal pressure gradients are very steep both in the radial and the x - direction in NPCH; so are the density gradients, although little milder.

The reasons why we did not consider the pressure force from the background plasma are, i) collisionless nature of the NPCH is well established and ii) NPCH fulfills the non-neutral plasma and One Component Plasma (OCP) conditions, i.e.,  $r_c \ll \lambda_D$  and  $L_T \geq \lambda_D$ ; where  $r_c$  is the Larmor radius of O VI ions,  $\lambda_D$  is the Debye length and  $L_T$  is the temperature length scale across the magnetic field (Dubin & O’Neill, 1997).

The crucial point is if the PCH could be regarded as a non-neutral plasma. Dubin & O’Neill (1999) points to the similarity between non-neutral plasma and OCP. Particle beams are used as a new application in non-neutral plasma experiments (Marler & Stoneking, 2007). O VI ions are preferentially heated species of NPCH plasma. Their effective temperature reaches to  $10^8$  K. This is at least two orders of magnitude higher than those of any other plasma species in the range 1.6 - 3.5 R. O VI ions may be regarded as “ion beams” in the quasi-neutral and immobile (with respect to O VI ions) NPCH background plasma as a non-neutral OCP.

We do not want to mislead the reader with the concept of “mobility”. It is a well established fact that NPCH is collisionless. Mobility is meaningful in a collisional plasma. In a neutral or quasi-neutral plasma electrons are more mobile, therefore in such media electron Debye length is used. On the other hand, in a collisionless plasma, “collision frequency”, “mean free path” and “collision time scale” appearing in the formula of the mobility lose their validities.

If we can consider the NPCH as a non-neutral OCP then only the ion Debye length should be used in the above two conditions, i.e.,  $r_c \ll \lambda_D$  and  $L_T \geq \lambda_D$ . Because electron Debye length is formulated under several assumptions: a) plasma is in a thermodynamic state; b) in case electron Debye length is considered then shielding is due to only one sign, i.e., electrons. This is a cold

ion approximation ( $T_i = 0$ ) wherein  $T = T_e$  is valid (Somov, 2006). Neither of the above two assumptions are justifiable in the NPCH. SoHO observations showed that more than 2000 plasma species co-exist with different temperatures in NPCH, besides their parallel and perpendicular (to the external magnetic field) velocities are quite different. Again, SoHO observations revealed that  $T_e \sim 10^5 - 10^6$  K but  $T_i^{OVI} \sim 5 \times 10^6 - 10^8$  K. In NPCH, electrons are too slow to shield O VI ions. With these observational data in hand, we may claim that short range collisions could occur only between O VI ions themselves, if at all.

Through the radial distance 1.6-3.0 R,  $r_c/\lambda_D$  changes from 0.061 to 0.095;  $L_T/\lambda_D$  changes from  $7 \times 10^4$  to  $1.81 \times 10^4$ , respectively. Therefore the quantitative criteria, i.e.,  $r_c \ll \lambda_D$  and  $L_T \geq \lambda_D$ , are fulfilled in the NPCH.

The  $\nabla n$  and  $\nabla T$  terms we consider are exclusively for the O VI ions, i.e., O VI ion number density as well as the perturbed part of the effective temperature variations in the radial and x - directions. Bearing all these in mind, we follow the Schekochihin et al. (2005) model and insert the pressure gradient term into the Vlasov equation. In this case the quasi-linearized Vlasov equation becomes,

$$\begin{aligned} \frac{df_1}{dt} = \frac{\partial f_1}{\partial t} + \mathbf{v} \cdot \frac{\partial f_1}{\partial \mathbf{R}} + \frac{q_i}{m_i} (\mathbf{E}_1 + \frac{1}{c}(\mathbf{v} \times \mathbf{B}_0)) \cdot \frac{\partial f_1}{\partial \mathbf{v}} = & \left[ -\frac{q_i}{m_i} (\mathbf{E}_1 + \frac{1}{c}(\mathbf{v} \times \mathbf{B}_1)) \right. \\ & \left. + \frac{k_B}{n_0 m_i} \left( T_{\text{eff}}^\xi \frac{\partial n_0}{\partial \mathbf{R}} + T_{\text{eff}}^\xi \frac{\partial n_0}{\partial \mathbf{x}} + n_0 \frac{\partial T_{\text{eff}}^\xi}{\partial \mathbf{R}} + n_0 \frac{\partial T_{\text{eff}}^\xi}{\partial \mathbf{x}} \right) \right] \cdot \frac{\partial f_0}{\partial \mathbf{v}} \end{aligned} \quad (12)$$

where  $f_0$  and  $f_1$  are the unperturbed and perturbed parts of the velocity distribution function, and  $\mathbf{E}_1$  and  $\mathbf{B}_1$  are the wave electric and magnetic fields, respectively. The time derivative is taken along the unperturbed trajectories in phase - space of O VI ions. Hereafter, for the sake of brevity, we'll designate the linearized form of the pressure force as,

$$\nabla p_1 = \frac{k_B}{n_0 m_i} \left( T_{\text{eff}}^\xi \frac{\partial n_0}{\partial \mathbf{R}} + T_{\text{eff}}^\xi \frac{\partial n_0}{\partial \mathbf{x}} + n_0 \frac{\partial T_{\text{eff}}^\xi}{\partial \mathbf{R}} + n_0 \frac{\partial T_{\text{eff}}^\xi}{\partial \mathbf{x}} \right) \quad (13)$$

Left circularly polarized ICW which interacts with the perturbed velocity distribution function is given by Schmidt (1979). Since we extend his study by taking the  $\nabla p$  term into account, the perturbed velocity function is modified as below,

$$f_L = -\frac{q_i}{m_i} \left[ \left( 1 - \frac{v_{\parallel} k}{\omega} \right) \frac{\partial f_0}{\partial v_{\perp}} + \frac{k v_{\perp}}{\omega} \frac{\partial f_0}{\partial v_{\parallel}} \right] E_x \exp(i\theta_0) \frac{1 - \exp \phi}{i(k v_{\parallel} - \omega + \omega_c)} + \nabla p_1 \quad (14)$$

where  $\theta_0$  is the initial phase of the wave and  $\phi = [i(k v_{\parallel} - \omega + \omega_c)(t - t_0)]$ .  $f_1$  produces a current the x - component of which is (*ibid*),

$$\begin{aligned} J_x = -\frac{q_i^2 \pi}{m_i \omega} E_x \int \frac{(\omega - k v_{\parallel})(\partial f_0 / \partial v_{\perp}) + k v_{\perp} (\partial f_0 / \partial v_{\parallel})}{k v_{\parallel} - \omega + \omega_c} (1 - \exp \phi) v_{\perp}^2 dv_{\perp} dv_{\parallel} \\ + i\pi q_i \int \nabla p_1(t - t_0) v_{\perp}^2 dv_{\perp} dv_{\parallel} \end{aligned} \quad (15)$$

$J_y$  component of the current is found in a similar manner. The result is  $J_x/E_x = J_y/E_y = \mathbf{J}/\mathbf{E}$ . The plasma dielectric tensor is obtained from the relation given below (e.g. Stix 1962)

$$\mathbf{J} + \frac{i\omega}{4\pi} \mathbf{E} = \frac{i\omega}{4\pi} \boldsymbol{\kappa} \cdot \mathbf{E} \quad (16)$$

Using Eq. (16) we obtain the dielectric tensor for the left circularly polarized ICW as below:

$$\begin{aligned} \kappa_L = 1 + 4\pi \frac{J_x/E_x}{i\omega} = 1 - \frac{4\pi^2 q_i^2}{im_i \omega^2} \int_{-\infty}^{+\infty} dv_{\parallel} \int_0^{\infty} \frac{(\omega - kv_{\parallel})(\partial f_0/\partial v_{\perp}) + kv_{\perp}(\partial f_0/\partial v_{\parallel})}{k v_{\parallel} - \omega + \omega_c} (1 - \exp \phi) v_{\perp}^2 dv_{\perp} \\ + \frac{4\pi^2 q_i}{\omega E_x} (t - t_0) \int_0^{\infty} \nabla p_1 v_{\perp}^2 dv_{\perp} dv_{\parallel} \end{aligned} \quad (17)$$

The dispersion relation for left circularly polarized ICW is obtained by  $\kappa_L = n^2 = c^2 k^2 / \omega^2$ , where  $n$  is the refractive index of the medium for ICW.

Bearing in mind the collisionless nature of the PCH and the observational fact that  $T_{\perp} \sim 10^2 T_{\parallel}$  we assumed that the velocity distribution function is bi-Maxwellian (see also Cranmer et al. 2008),

$$f_0 = n_i \alpha_{\perp}^2 \alpha_{\parallel} \pi^{-3/2} \exp \left[ - \left( \alpha_{\perp}^2 v_{\perp}^2 + \alpha_{\parallel}^2 v_{\parallel}^2 \right) \right] \quad (18)$$

where  $\alpha_{\perp} = (2k_B T_{\perp} / m_i)^{-1/2}$  and  $\alpha_{\parallel} = (2k_B T_{\parallel} / m_i)^{-1/2}$  are the inverse of the most probable speeds in the perpendicular and parallel direction to the external magnetic field, respectively.  $\partial f_0 / \partial v_{\perp}$  and  $\partial f_0 / \partial v_{\parallel}$  appearing in Eq. (17) will be derived from Eq. (18). We should remind the reader that  $[\mathbf{E} + \frac{1}{c} \mathbf{v} \times \mathbf{B}_0 - \nabla p] \cdot \nabla_v f$  term in the Vlasov equation is a non-linear term, therefore harbours non-linear effects like the ICR process. This property of the velocity distribution function makes the approximation quasi-linear. We may justify this assumption on the ground that, quasi-linear theory provides an accurate description for small amplitude waves. In this small amplitude limit, exchange of energy between waves and particles are well quantified (e.g. Goldston & Rutherford 1995; Gurnett & Bhattacharjee 2005). Cranmer (2000) also considered small amplitude waves in a collisionless, homogeneous plasma wherein he points to the fact that in this ideal case dissipation of ICW occurs via ICR. In this investigation, we depart from the homogenous case and consider all the gradients of plasma parameters which are observationally revealed. When we substitute the  $\partial f_0 / \partial v_{\perp}$  and  $\partial f_0 / \partial v_{\parallel}$  into Eq. (17) we get the contribution of the principle integral to the dispersion relation of ICW as below,

$$\begin{aligned} k^2 \left( c^2 - \frac{\omega^2}{k^2} \right) - \frac{i\omega_p^2 \omega}{(\omega - \omega_c)} - \frac{i\omega_p^2 k}{\sqrt{\pi} \alpha_{\parallel} (\omega - \omega_c)} \left( \frac{T_{\perp}}{T_{\parallel}} + \frac{\omega}{(\omega - \omega_c)} - 1 \right) \\ - \frac{i\omega_p^2 k^2}{2\alpha_{\parallel}^2 (\omega - \omega_c)^2} \left( \frac{\omega}{(\omega - \omega_c)} + \frac{T_{\perp}}{T_{\parallel}} - 1 \right) + \frac{\pi^2 \omega q_i L}{E_x v_A} \nabla p_1^r = 0 \end{aligned} \quad (19)$$

where  $\omega_p = (4\pi n_{OVI} q_i^2 / m_i)^{1/2}$  is the plasma frequency for the O VI ions and  $\nabla p_1^r$  is the term designating rather lengthy pressure gradient in its reduced form:

$$\nabla p_1^r = \frac{k_B}{m_i} \left[ \left( T_{\text{eff}}^{\xi} \frac{\partial n_0}{\partial R} + n_0 \frac{\partial T_{\text{eff}}^{\xi}}{\partial R} \right) \left( \frac{T_{\perp}}{T_{\parallel}} \right)^{1/2} + 2 \left( T_{\text{eff}}^{\xi} \frac{\partial n_0}{\partial x} + n_0 \frac{\partial T_{\text{eff}}^{\xi}}{\partial x} \right) \right] \quad (20)$$

We put  $L/v_A$  instead of the time interval term  $t - t_0$  in Eq. 17, where  $L$  is the displacement of a wave (3.5-1.5 R) and  $v_A$  is the Alfvén speed, i.e.,  $v_A = B(R)/(4\pi n_i m_i)^{1/2}$ . Hereafter, for the sake of brevity we replace  $[\omega/(\omega - \omega_c)] + (T_{\perp}/T_{\parallel}) - 1$  by  $\Pi$  which stands for the principle contribution.

The residual contribution is:

$$\mathfrak{R} = \frac{2\sqrt{\pi}\omega_p^2}{k} \alpha_{\parallel} \left[ \omega_c + (\omega - \omega_c) \frac{T_{\perp}}{T_{\parallel}} \right] \exp \left[ -\alpha_{\parallel}^2 \left( \frac{\omega - \omega_c}{k} \right)^2 \right] \quad (21)$$

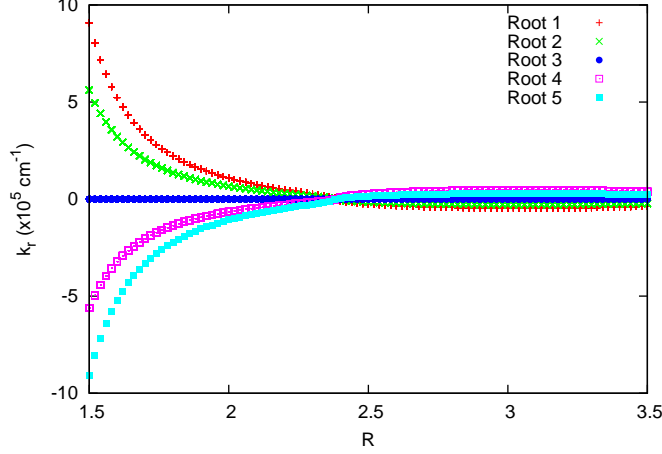


Figure 2: All five roots of the fifth order dispersion relation given by Eq. 23. Roots 1, 2, 4 and 5 represent the forward propagating modes, and root 3 is the backward propagating mode.

Combination of the Eqs (19) and (21) is the dispersion relation for the ICW in PCH,

$$\begin{aligned}
 & k^2 \left( c^2 - \frac{\omega^2}{k^2} \right) - \frac{i\omega_p^2}{(\omega - \omega_c)} \left[ \omega + \frac{k}{\sqrt{\pi}\alpha_{\parallel}} \Pi + \frac{k^2}{2\alpha_{\parallel}^2 (\omega - \omega_c)} \Pi \right] \\
 & + \frac{\pi^2 \omega q_i L}{E_x v_A} \nabla p_1^r - \frac{2\sqrt{\pi}\omega_p^2}{k} \alpha_{\parallel} \Phi \exp \left[ -\alpha_{\parallel}^2 \left( \frac{\omega - \omega_c}{k} \right)^2 \right] = 0
 \end{aligned} \tag{22}$$

where  $\Phi = [\omega_c + (\omega - \omega_c)T_{\perp}/T_{\parallel}]$ . If we expand the exponential factor appearing in the last term of the Eq. (22) into Taylor series, we obtain the *dispersion relation I* (DR I) as below,

$$\begin{aligned}
 & k^5 \left[ c^2 - \frac{i\omega_p^2}{2\alpha_{\parallel}^2 (\omega - \omega_c)^2} \Pi \right] - k^4 \frac{i\omega_p^2}{\sqrt{\pi}\alpha_{\parallel} (\omega - \omega_c)} \Pi - k^3 \left[ \omega^2 + \frac{i\omega_p^2 \omega}{(\omega - \omega_c)} - \frac{\pi^2 \omega q_i L}{E_x v_A} \nabla p_1^r \right] \\
 & - k^2 2\sqrt{\pi}\omega_p^2 \alpha_{\parallel} \Phi + 2\sqrt{\pi}\omega_p^2 \alpha_{\parallel}^3 (\omega - \omega_c)^2 \Phi = 0
 \end{aligned} \tag{23}$$

The graphical solution of the Eq. (23) (DR I) is given in Figure 2. Whitelam et al. (2002) investigated the theoretical models that may explain the formation of small scale jet-like structures known as spicules and macrospicules in the solar transition region. In their ponderomotive force acceleration model, they found that in order to achieve accelerations of the order of  $1 \text{ km s}^{-2}$ , an Alfvén wave with a field strength of order  $E \approx 8 \text{ V m}^{-1}$  is required (see their Eq. 16). We use this value for the  $E_x$  term in our equations. Terradas et al. (2010) investigated the resonant absorption of the fundamental kink mode in a coronal loop. They showed that the system becomes unstable when the frequencies of the forward and the backward propagating waves merge. We obtained a similar result, although our DR is solved for real frequency and complex  $k$ , the wave number. Waves in a lossy medium are identified with respect to the analytical form of complex valued wave numbers, i.e.,  $k = k_r + ik_i$ . We assumed that the field function of the wave is of the form,  $\exp[i(\mathbf{k} \cdot \mathbf{r} - \omega t)] = \exp[i(\mathbf{k}_r \cdot \mathbf{r} - \omega t)] \exp(-\mathbf{k}_i \cdot \mathbf{r})$ . If the solution of the dispersion relation yields  $k_i > 0$  then the wave damps in the  $\mathbf{r}$ -direction. Damping occurs if the energy flux of the wave is

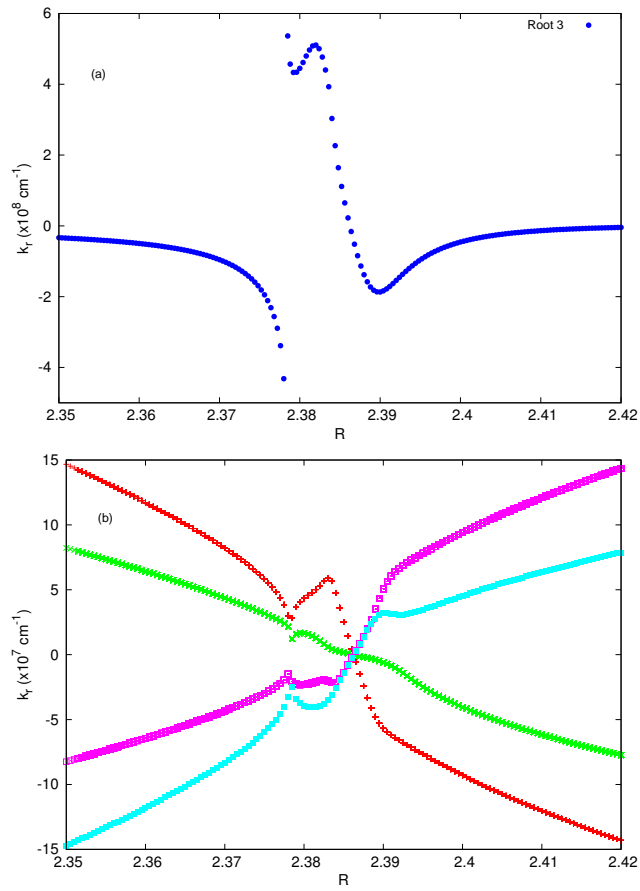


Figure 3: (a) Root 3 only. This root represents the mode resonating with OVI ions at about  $R = 2.38$ ; (b) Roots 1,2,4 and 5 in the reflection region. In the close vicinity of  $R = 2.39$  fast and slow modes are reflected, i.e. wavenumbers become zero. The graphs are for ICW with a frequency  $2500 \text{ rads}^{-1}$ .

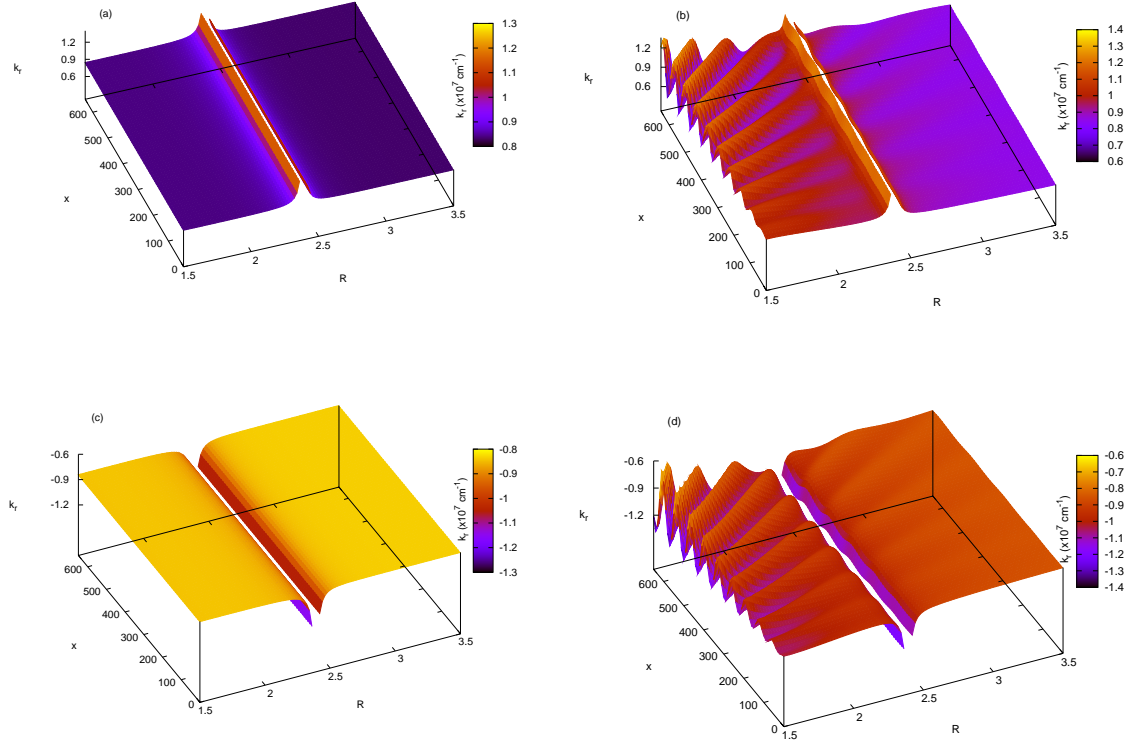


Figure 4: Two roots of the second order dispersion relation given by Eq. (24). (a) Forward propagating mode when the gradients of plasma parameters are not taken into account; (b) the same mode with gradients considered; (c) backward propagating mode without gradients and (d) the same mode with gradients considered. The graphs are for ICW with a frequency  $2500 \text{ rads}^{-1}$ . The higher values of  $k_r$  in interplume lanes reveals higher refractive index ( $n = ck_r/\omega$ ) which in turn, points to the more effective wave-particle interaction and thus resonance.

also in the  $\mathbf{r}$ -direction. Shevchenko (2007) introduces a criterion that helps to identify the waves, that is,  $\text{Im}k^2 = 2k_r k_i \gtrless 0$  where the upper (lower) sign is for the backward (forward) wave. Our dispersion relation has five roots, 4 of which is forward and the one of which is backward.

Figure 2 shows that forward and backward propagating fast and slow modes with a frequency of  $2500 \text{ rads}^{-1}$  merge at about  $2.38 R$ . We'll show in the Figure 3 that this location is the site where ion cyclotron resonance and cut-offs take place in a small range of distance. In Fig. 3a only the third root of DR I is shown. This root reveals a resonance at about  $R = 2.38$ . The other four roots (Root 1,2,4 and 5) are given in Fig 3b. A reflection of the slow and fast modes occurs at  $R=2.39$ . We should emphasize that the reflection site and the resonance site are not coincident.

We should also remind the reader that the Taylor series approximation is valid only in the close vicinity of the resonance region, i.e.  $R=2.38$  for the frequency  $\omega = 2500 \text{ rads}^{-1}$ . Therefore our approximation for DR I would be invalid in the regions away from the resonance.

From the solution of DR I we find that the wave numbers are of the order of  $10^{-8} - 10^{-7} \text{ cm}^{-1}$

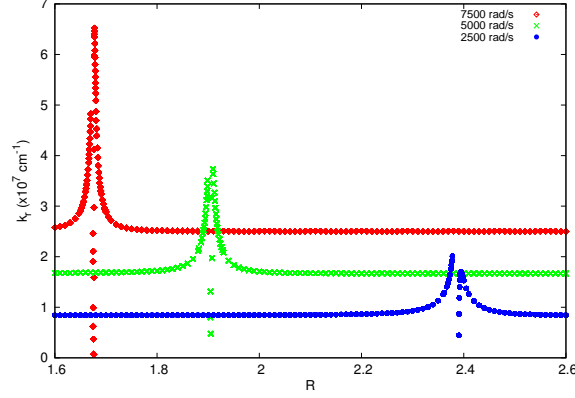


Figure 5: This is the  $(R, k_r)$  version of Figure 3 (a). A local maximum is apparent close to the  $R = 2.4$ . At  $R = 2.38$  the wave resonate with and transfer its energy to OVI ions.

at the resonance site. By putting this value into Eq. (21) we see that the highest value of the residual contribution turns out to be  $10^{-5}$ . This is negligibly small compared to the values of the rest of the terms which range between  $10^6 - 10^{13}$  in the Eq. (22), so we can neglect it. In this case, DR I given by the Eq. (23) is reduced to DR II given by the Eq. (24) below,

$$k^2 \left[ c^2 - \frac{i\omega_p^2}{2\alpha_{\parallel}^2 (\omega - \omega_c)^2} \Pi \right] - \frac{i\omega_p^2 k}{\sqrt{\pi} \alpha_{\parallel} (\omega - \omega_c)} \Pi - \frac{i\omega_p^2 \omega}{(\omega - \omega_c)} - \omega^2 + \frac{\pi^2 \omega q_i L}{E_x v_A} \nabla p_1^r = 0 \quad (24)$$

The graphical solution of the Eq. (24) is given in Figure 4. The solution of DR II gives the values of  $k$  of about  $10^{-7} \text{ cm}^{-1}$ . With this  $k$  value the residual contribution becomes even more negligible. But we happened to show, *a posteriori*, that the residual contribution can safely be neglected. Figure 4a is the solution of the Vlasov equation not including the  $-\nabla p$  force. The solution reveals an infinity in the refractive index, corresponding to a resonance, throughout the region considered at about  $2.38 R$ . In this case, refractive index in  $(R, x)$  domain has the same value, before and after the  $2.38 R$  where it becomes infinity. When we take the PIPL structure into account, the infinity in the refractive index persists in the same  $2.38 R$  distance but the differences in the refractive index of the plumes and interplume lanes are also revealed (Fig. 4b). Figure 4b shows the crests and the troughs in the refractive index, the former corresponds to the interplume lanes and the latter to the plumes. We may argue that the refractive index of the interplume lanes is readily going to infinity indicating that the resonance process in the interplume lanes is more effective than in the plumes. This result is confirmed by the observations showing that the source of the fast solar wind is interplume lanes.

Figure 5 is the  $(R, k_r)$  version of Figure 4a. A local maximum is apparent close to the  $R = 2.4$ . At  $R = 2.38$  the wave resonate with and transfer its energy to OVI ions. The pattern seen in Figure 4 is also visible in Figure 4(a,b,c,d). In the wave-particle interaction context, one cannot consider a single wave frequency but a band of frequencies. Therefore, we assumed the presence of ICW in PCH generated with a frequency range of  $2500 - 10000 \text{ rads}^{-1}$ . The waves with frequencies higher than  $2500 \text{ rads}^{-1}$  hit their magnetic beaches at smaller  $R$  and the ones with frequencies lower than  $2500 \text{ rads}^{-1}$  at greater  $R$  distances (see Fig.4).

We should mention, in passing, that when we adopt  $10^{-3}$  for  $N_{OVI}/N_p$ , which is the value Vocks (2002) used in his model for the kinetics of ions in the solar corona, the ratio of the wave numbers  $k_{\nabla p}/k$  range from 0.2 to 16.8 in the distance range 1.5-3.5 R, where  $k_{\nabla p}$  is the wave number of the waves propagating in the presence of gradients considered, i.e.  $\nabla T_{eff}^{\xi}(R, x), \nabla n(R, x)$ . For  $N_{OVI}/N_p = 1.52 \times 10^{-6}$  which is the value given by Cranmer et al. (2008),  $k_{\nabla p}/k$  take values between 0.7 and 1.6. We plotted the figures by adopting the later value, i.e. Cranmer et al.'s (2008). Despite the three orders of magnitude difference in O VI abundances given in the above two references, it is apparent that gradients both in x and R direction of plasma parameters shortens the wavelength of the waves.

Finally, after having obtained wave numbers by solving the DRI and DRII, we checked if the second condition for *cold plasma* approximation, i.e.,  $v_{\parallel} \ll \omega/k_{\parallel}$ , holds true. For ion thermal velocity we take the parallel component of the bi-Maxwellian distribution function given in Eq. (18), that is,  $\alpha_{\parallel}^{-1} = (2k_B T_{\parallel}/m_i)^{1/2}$ , and for the parallel phase velocity,  $\omega/k_{\parallel}$ , where  $\omega$  is assigned a value in the range  $2500 \text{ rads}^{-1} < \omega < 10000 \text{ rads}^{-1}$  and  $k_{\parallel}$  are derived from DRI and DRII. With these values, we obtained that  $v_{\parallel}/(\omega/k_{\parallel}) \sim 10^{-3}$ . This condition is fulfilled also for the whole frequency range.

#### 4. Conclusions

In the present investigation, the response of O VI ions to ICW in the PCH is studied. When the wave frequency is equal to the ion cyclotron frequency, i.e.,  $\omega = \omega_c$ , LCP waves transfer their energy to the O VI ions. This is true for all the ions, but O VI ions are preferentially heated.

All the PCH plasma parameters,  $N_e, N_p, N_{OVI}, B, T_{eff}, T_{eff}^{\xi}$  obtained by SoHO, are functions of the radial as well as the  $x$ -direction. This property of the medium makes the refractive index a function of position. When the wave frequency approaches to the ion cyclotron frequency ICR process takes place and the wave energy is transferred to the O VI ions. This is revealed by the value of the refractive index going, in a jumpy manner, to infinity. Energy transfer from ICW to O VI ions is in such a way as to increase the perpendicular velocity in their helical trajectory around the magnetic field. This causes the violation of the first adiabatic invariant, the magnetic moment, and increases the magnetic mirror force, consequently accelerate OVI ions in radial direction. Inclusion of  $\nabla p$  in DR I doesn't significantly alter the solution, but it is otherwise for DR II. As it is apparent from the figures that refractive index in the interplume lanes are about 2 times higher than the ones in the plumes. This result of ours is confirmed by the observational data that the seat of the fast solar wind is interplume lanes. For instance, Prasad et al. (2011) by using high spatial and temporal resolution of AIA/SDO, searched for the wave-like disturbances in plumes and interplume lanes in PCH. They concluded that wave propagation speeds are higher in the interplume lanes than those of plumes.

We showed that for propagation parallel to the magnetic field in PCH, infinities in  $n_{\parallel}^2$  occur at ion cyclotron frequency. Now, considering the ICW with a frequency  $2500 \text{ rads}^{-1}$  propagating towards weakening magnetic field, i.e., from the coronal base out to the extended corona in radial direction, it is apparent from Figure 3a that wave frequency approaches to the local cyclotron frequency. Dispersion relation then yields larger  $k_{\parallel}$  values with  $k_i > 0$  which indicate the absorption of ICW through cyclotron damping. The geometry of this process is referred to as *magnetic beach* (Stix, 1992).

In this investigation, we tried to show that ICR process can heat one of the ion species, i.e. OVI. Although we consider a single ion species, this process seems to hold true for other ion



species as well.

## Acknowledgments

The authors acknowledge and thank an anonymous referee, E.Devlen, K.Yakut and D.Cole for their useful suggestions and comments. Our special thanks go to copyright holder of Figure 1 in the present study, i.e., Wiley-VCH GmbH & Co. KGaA and the authors of the paper (E.Devlen & E.R.Pekünlü, 2010, *Astron Nachr.*, 331, 716). Figure 1 is reproduced with their kind permission. SD appreciates the support by the Turkish Academy of Sciences (TÜBA) Doctoral Fellowship. This study is a part of PhD project of SD.

## References

- Antonucci, E., Dodero, M. A., & Giordano, S. 2000, *SoPh*, 197, 115  
Axford, W. I., McKenzie, J. F., Sukhorukova, G. V. et al. 1999, *SSRv*, 87, 25  
Banerjee, D., Teriaca, L., Doyle, J. G. et al. 1998, *A&A*, 339, 208  
Banerjee, D., Teriaca, L., Doyle, J. G. et al. 2000, *SoPh*, 194: 43- 58  
Banerjee, D., Teriaca, L., Gupta, G. R., Imada, S., Stenborg, G., & Solanki, S. K. 2009, *A&A*, 499, L29  
Banerjee, D., Pérez-Suárez, D., & Doyle, J. G. 2009, *A&A*, 501, L15  
Cheng, C.Z. 1991, *JGR*, 96, No. A12, 159 - 171  
Cheng, C.Z. 1999, *JGR*, 104, No. A1, 413-427  
Ciaravella, A., Raymond, J. C., Strachan, L. et al. 1999, *ApJ*, 510, 1053  
Cranmer, S. R., Field, G. B., & Kohl, J. L. 1999, *SSRv*, 87, 149  
Cranmer, S. R. 2000, *ApJ*, 532, 1197  
Cranmer, S. R. 2002, *SSRv*, 101, 229  
Cranmer, S. R., Panasyuk, A. V., & Kohl, J. L. 2008, *ApJ*, 678, 1480  
Devlen, E., & Pekünlü, E. R. 2010, *AN*, 331, 716  
Doorselaere, T. V., & Nakariakov, V. M. 2008, *First Results From Hinode ASP Conference Series*, Vol. 397,58  
Doyle, J. G., Teriaca, L., & Banerjee, D. 1999, *A&A*, 349, 956  
Dubin, D. H. E., & O'Neil, T. M. 1997, *Phys. Rev. Lett.*, 78, 3868  
Dubin, D. H., & O'neil, T. M. 1999, *Rev. Mod. Phys.*, 71, 87  
Endeve, E., & Leer, E. 2001, *SoPh*, 200, 235  
Esser, R., Fineschi, S., Dobrzycka, D. et al. 1999, *ApJ*, 510, L63  
Fisher, R., & Guhathakurta, M. 1995, *ApJ*, 447, L139  
Gupta, G. R., Banerjee, D., Teriaca, L., Imada, S., & Solanki, S. 2010, *ApJ*, 718, 11  
Goldston, R.J., & Rutherford, P.H. 1995, *Introduction to Plasma Physics*, Institute of Physics Press, Bristol  
Gurnett, D.A., & Bhattacharjee 2005, A., *Introduction to Plasma Physics: with space and laboratory applications*, Cambridge University Press, Cambridge  
Hollweg, J. V. 1999a, *JGR*, 104, 24781  
Hollweg, J. V. 1999b, *JGR*, 104, 24793  
Hollweg, J. V. 1999c, *JGR*, 104, 505  
Isenberg, P. A., & Vasquez, B. J. 2009, *ApJ*, 696, 591  
Joarder, P. S., Nakariakov, V. M., & Roberts, B. 1997, *SoPh*, 176, 285  
Kohl, J. L., Noci, G., Antonucci, E. et al. 1997a, *SoPh*, 175, 613  
Kohl, J. L., Noci, G., Antonucci, E. et al. 1997b, *AdSpR*, 20, 3  
Kohl, J. L., Esser, R., Cranmer, S. R. et al. 1999, *ApJ*, 510, L59  
Kohl, J. L., Noci, G., Cranmer, S. R., & Raymond, J. C. 2006, *A&ARv*, 13, 31  
Kumar, N., Kumar, P., & Singh, S. 2006, *A&A*, 453, 1067  
Lie-Svendsen, Ø., Hansteen, V. H., Leer, E., & Holzer, T. E. 2002, *ApJ*, 566, 562  
McIntosh, S. W., de Pontieu, B., Carlsson, M., Hansteen, V., Boerner, P., & Goossens, M. 2011, *Nature*, 475, 477  
Marler, J. P., & Stoneking, M. R. 2007, *JPhCS*, 71, 012003  
Marsch, E. 1999, *SSRv*, 87, 1  
Marsch, E., & Tu, C.-Y. 1997, *A&A*, 319, L17  
Melrose, D.B. & McPhedron 1991, R.C. *Electromagnetic processes in dispersive media*, Cambridge University Press  
Murawski, K., Oliver, R., & Ballester, J. L. 2001, *A&A*, 375, 264

Nakariakov, V. M., Roberts, B., & Murawski, K. 1998, *A&A*, 332, 795  
 Nakariakov, V. M. 2006, *Royal Society of London Philosophical Transactions Series A*, 364, 473  
 Ofman, L., Nakariakov, V. M., & Sehgal, N. 2000, *ApJ*, 533, 1071  
 Pekünlü, E. R., Yakut, K., & Sart, H. 2004, *Turkish Journal of Physics*, 28, 407  
 Prasad, S.K., Banerjee, D., & Gupta, G. R. 2011, *A&A*, 528, L4  
 Raymond, J. C., Kohl, J. L., Noci, G. et al. 1997, *SoPh*, 175, 645  
 Ruderman, M. S., Oliver, R., Erdélyi, R., Ballester, J. L., & Goossens, M. 2000, *A&A*, 354, 261  
 Schekochihin, A.A., Cowley, S.C., Kulsrud, R.M., Hammett, G.W., & Sharma, P. 2005, *ApJ*, 629, 139  
 Schmidt, G., *Physics of High Temperature Plasmas*, 2nd. ed., Academic Press, New York, 1979  
 Shevchenko, V.V. 2007, *Physics - Uspekhi* 50 (3) 287-292  
 Somov, B. V. 2006, *Plasma Astrophysics, Part I*, Berlin: Springer  
 Stix, T.H. 1962, *The Theory of Plasma Waves*, McGraw - Hill Book Co., New York  
 Stix, T. H. 1992, *Waves in Plasmas*, Springer  
 Terradas, J., Goossens, M., & Ballai, I. 2010, *A&A* 515, A46  
 Tomczyk, S., McIntosh, S. W., Keil, S. L. et al. 2007, *Science*, 317, 1192  
 Tronci, C., 2010, *JPhA*, 43,5501  
 Tu, C.-Y., & Marsch, E. 1997, *SoPh*, 171, 363  
 Tu, C.-Y., & Marsch, E. 1999, *American Institute of Physics Conference Series*, 471, 373  
 Vocks, C., & Marsch, E. 2001, *GRL*, 28, 1917  
 Vocks, C. 2002, *ApJ*, 568, 1017  
 Voitenko, Y., & Goossens, M. 2002, *SoPh*, 206, 285  
 Whitelam, S., Ashbourn, J. M. A., Bingham, R. et al., 2002, *SoPh*, 211, 199  
 Wilhelm, K., Marsch, E., Dwivedi, B. N. et al. 1998, *ApJ*, 500, 1023  
 Wilhelm, K., Dammasch, I. E., Marsch, E., & Hassler, D. M. 2000, *A&A*, 353, 749  
 Williams, L. L. 1997, *ApJ*, 481, 515